

---

Article

# Inactivating SARS-CoV-2 using 275nm UV-C LEDs through a spherical irradiation box: design, characterization and validation

Nicola Trivellin <sup>1</sup>, Matteo Buffolo <sup>2</sup>, Francesco Onelia <sup>3</sup>, Alberto Pizzolato <sup>4</sup>, Marco Barbato <sup>4</sup>, Viviana Teresa Orlandi <sup>5</sup>, Claudia Del Vecchio <sup>3</sup>, Fabrizio Dughiero <sup>1</sup>, Enrico Zanoni <sup>2</sup>, Gaudenzio Meneghesso <sup>2</sup>, Andrea Cristanti <sup>3</sup>, Matteo Meneghini <sup>2</sup>

<sup>1</sup>Department of Industrial Engineering, University of Padova, Via Gradenigo 6A, 35131 Padova (PD) Italy

<sup>2</sup>Department of Information Engineering, University of Padova, Via Gradenigo 6B, 35131 Padova (PD) Italy

<sup>3</sup>Department of Molecular Medicine, University of Padova, Via Gabelli 63, 35121 Padova (PD) Italy

<sup>4</sup>LightCube SRL, Viale Navigazione Interna 51, 35129, Padova (PD), Italy

<sup>5</sup>DBSV, University of Insubria, Via J.H. Dunant 3, 21100 Varese (VA), Italy

\* Correspondence: nicola.trivellin@unipd.it

**Abstract:** We report on the design, characterization and validation of a spherical irradiation system for inactivating SARS-CoV-2, based on UV-C 275 nm LEDs. The system is designed to maximize irradiation intensity and uniformity, and can be used for irradiating a volume of 18 liters. To this aim: (i) several commercially available LEDs have been acquired and analyzed; (ii) a complete optical study has been carried out in order to optimize the efficacy of the system. (iii) The resulting prototype has been characterized optically, and tested for the inactivation of SARS-CoV-2 for different exposure times, doses and surface types. Results indicate that a 99.9% inactivation can be reached after 1 minute of treatment with a dose of 83.1 J/m<sup>2</sup>.

**Keywords:** SARS-CoV-2, Covid-19, LED, UVC, disinfection, inactivation, virucide.

---

## Introduction

The spread of SARS-CoV-2 virus, the etiological agent of COVID-19, is stressing the global healthcare [1] and economical systems [2]. Although still discussed, the infection is thought to be mainly related to droplets and aerosol [3]. While personal devices like face masks are effective toward the spread of droplets [4] [5,6] contamination of surfaces [7], water and air must be prevented to minimize the spread of the virus. In most cases, decontamination is performed through chemical agents, like alcohol- or chlorine-based solutions. However, these disinfection strategies are time-consuming, and not suitable for large surfaces.

For this reason, non-chemical and photoassisted strategies are currently being explored, mostly based on ultraviolet light. Several papers indicated that UV light can be effective towards the inactivation of different pathogenic microorganisms, including, recently, the SARS-CoV-2 [8] on surfaces. The ability of having a precise and reliable sanitification can be achieved by UVC irradiation, thus helping the use of "community" objects like portable payment terminals, handrails, elevators, etc.

UV-assisted disinfection is of particular importance in community environments, especially in presence of young generations: schools, gyms and sport fields are often kept open to relieve social tension, thus being places where the virus can easily spread. In addition, team sport activities are affected by the necessary use of "community" objects like sport balls, that are touched by all players, in presence of droplets, aerosol and body fluids. For this reason, providing frequently sanitized sport equipment (like sport basketballs) is crucial for the containment of the contagion and the continuation of the

physical activities. Most personal objects used at school have dimensions of 100-200 mm, while sport-balls can have a diameter near 250 mm, so designing systems capable of inactivating the viruses in volumes around 15-18 liters is a necessity to control the virus in community life.

Deep ultraviolet LEDs based on Aluminum Gallium Nitride (AlGaN) material have been available since approximately two decades [9], nevertheless their limited performances [10], reliability [11] and high cost per watt were playing a major role in limiting their market diffusion. Recently, the efficiency of these devices has rose up to levels of 1-3%, while a sensible reduction of cost made them suitable for different commercial applications. UVC LEDs are still less efficient than low pressure mercury lamp, but their compactness, low voltage operation and instant switch on compensate for these deficiencies.

The goal of this paper is to present the design, optimization and validation of a sanification system based on UVC-LEDs, specifically tested with reference to SARS-CoV-2 virus. The proposed system is designed to inactivate the virus located on the surface of personal and community objects, in particular spherical sport balls, thus being ideal for the disinfection in community environments (sport field, school, ...).

### Experimental details

The light-emitting part of the system is represented by commercially available off-the-shelf UVC LEDs. For the proposed study we evaluated 6 UVC LEDs from different manufacturers, the details of the LEDs, as determined from each datasheet, are reported in Table I.

Table I: LED selection and properties

Manufacturer	LED Code	Nominal current $I_N$ (mA)	Nominal flux @ $I_N$ (mW)	Nominal wavelength (nm)	Maximum current (mA)	Voltage $V_f$ (V)
A	A1	20	2-4	270-280	40	6.5
A	A2	350	37.5	275	800	6.5
A	A3	350	37.5	280	800	6.5
B	B1	150	7.5	278	150	7.5
C	C1	100	10	275	150	6.3
D	D1	50	5	278	100	6.1

UVC LED technology is still under development. From the technical and cost/manufacturing aspects it becomes crucial to carefully estimate the electrical and optical properties of the available LEDs as a starting point for the design optimization.

In this work we performed: i) electrical characterization by means of current-voltage characteristics, ii) optical characterization by means of absolute spectral measurement; iii) efficiency analysis at different driving currents.

The electrical characterization was carried out by means of a Keithley 2614B Source-meter analyzer. For each LED, the voltage was swept between -2 V and the maximum rated voltage. The optical characterization was carried out by means of an absolute irradiance calibrated Ocean Insight USB4000 spectrometer equipped with a CC3-DA cosine corrector, the spectral range is between 200 and 850 nm. In order to perform the optical flux measurement, the LEDs were mounted on a 2 axis stepper motor goniometer and rotated in order to calculate the radiated flux from irradiance measurements. To acquire a sufficient signal from the LEDs the aperture of the spectrometer has been positioned at a distance of 300 mm from the emitter. The power emitted from the LED has also been measured at different current levels, in order to extract the efficiency of the different devices as a function of driving current.

The design of the irradiation chambers has been carried out by means of ray tracing simulations. For the implementation of the sources a rayfile has been calculated from the angular emission of the LEDs as previously measured. The optical simulations are aimed at calculating the spatial resolved irradiance on a sensor surface. The surface is shaped as the target object: a sphere, representing the largest object to be irradiated (sportsball).

The material and relative surface reflectivity used in the simulation is a steel surface covered with chromium, from the work of Sarosi et al. [12] we estimate a reflectivity of 60% at 275 nm. Distributing uniformly points on the surface of a sphere is a well-known problem with no perfect solution. The Matlab function `ParticleSampleSphere` [13] has been used to generate an approximately uniform triangular tessellation of a unit sphere (used at the beginning for minimizing the generalized electrostatic potential energy, i.e., Reisz  $s$ -energy, of a system of charged particles). Effectively, this function uses gradient descent and produces a locally optimal solution to the problem that involves finding a minimum Reisz  $s$ -energy configuration of  $N$  equally charged particles confined to the surface of a unit sphere. Initial configuration of particles is based on random sampling of a sphere.

Figure 1 reports the point distributions as calculated by the Matlab function and used in the following of this work for the design of a spherical emitting surface.

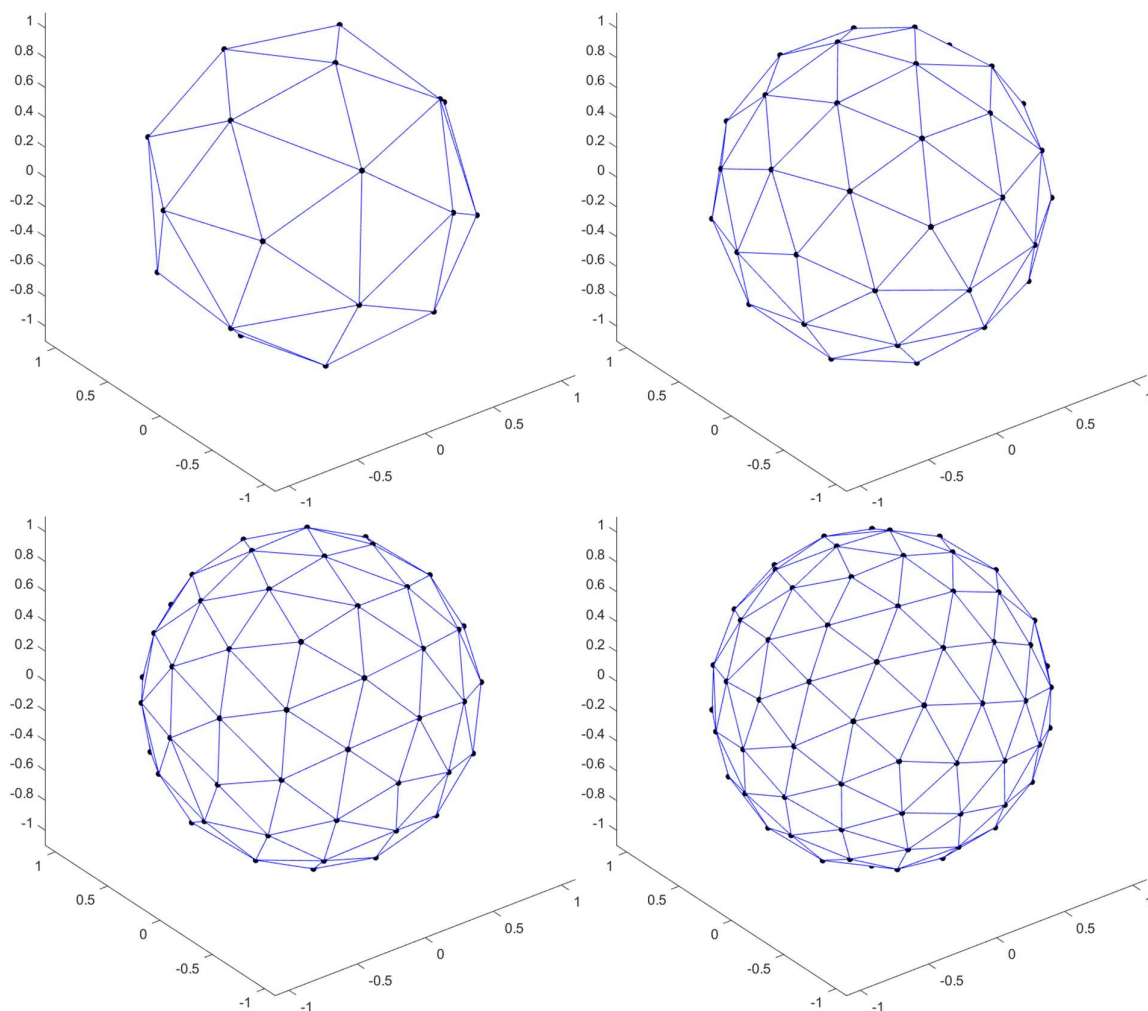


Figure 1: Calculated point distribution on the surface of a sphere (top left) 25 points, (top right) 50 points, (bottom left) 75 points, (bottom right) 100 points.

### Design target

When the wavelength is fixed, the antiviral effectiveness of a UV system is related to a specific irradiation fluence, corresponding to a specific light energy per unit area. The final aim of this design is to guarantee that in nearly the entirety of the irradiated object surface reaches a minimum fluence. Considering that for the type of the systems analyzed in this work the irradiation time is the same for the entire target surface, a minimum fluence value translates into a minimum irradiance value.

In both systems the target of the design is an optimization of the minimum irradiance on the target surface versus the cost of the system. For this analysis the cost of the system is represented mainly by the cost of the single LED multiplied by the number of the LEDs in the system. On the market, LEDs emitting at a peak wavelength of  $275 \pm 10$  nm are available with different radiant fluxes, typical values go from 10 mW for a 100 mA device to 110 mW for a 800 mA device. Considering that the price of these LEDs ( $Price_{LED}$ ) increases with their emitted optical power ( $OP_{LED}$ ) with a nearly linear dependence (defined  $K_p$  factor in the following), we estimate that the price of the system ( $Price_{sys}$ ) composed of  $N$  LEDs is related to the total optical power ( $OP_{sys}$ ) emitted and that the LEDs all have the same power.

$$OP_{sys} = N * OP_{LED} \quad (1)$$

$$Price_{LED} = K_p * OP_{LED} \quad (2)$$

$$Price_{sys} = N * Price_{LED} = N * K_p * OP_{LED} = K_p * OP_{sys} \quad (3)$$

For a finer assessment of the costs, one should consider that, by increasing the number of LEDs an intrinsic higher manufacturing and assembly cost: we will therefore carefully optimize their number.

For a fixed treatment time, the design rule becomes to obtain a minimum irradiance for a given total installed power. Since a local irradiance higher than the minimum is not necessary, the immediate annotation is that to improve the minimum irradiance we should also improve the irradiance uniformity, in order not to waste any optical power.

#### Optical design

From recent scientific literature, the amount of fluence necessary to inactivate the Sars-CoV-2 is estimated at different values approximately between 6-8 mJ/cm<sup>2</sup> [14], up to 37.5 mJ/cm<sup>2</sup> [15] Our aim is to inactivate the virus in few minutes, possibly just 60 seconds. We set the ideal average irradiance at 2.5 W/m<sup>2</sup> and a target minimum irradiance of 1 W/m<sup>2</sup>. The ideal average irradiance does not consider the actual optical losses, while the minimum irradiance is the target value for the optimization we will use in the following.

In the design of the system, several possible architectures have been evaluated, but for manufacturing simplicity a design constraint has been set: LEDs are positioned onto a spherical surface with a diameter of 330 mm, the optical axis of each LED is pointing at the center of the sphere. We will optimize the number of the LEDs together with their optical power. The uniformity will be evaluated for 25, 50, 75 and 100 LEDs, while the sum of the power emitted by the LEDs will be approximately 500 mW. We will also investigate the effect of the diameter of the internal sphere with respect to irradiance values. The best optimization solution will be the configuration allowing the higher minimum value of irradiance.

To analyze the data we will use, among others, the non-uniformity NU parameter, defined as reported below:

$$NU = \frac{E_{max} - E_{min}}{E_{max} + E_{min}} \times 100 [\%] \quad (4)$$

## Biological materials and assays

### *Viral stock preparation and viral titer evaluation*

The photoinactivation tests have been performed against virus belonging to family of *Coronaviridae*, SARS-CoV-2. All the experiments were performed in a biosafety level 3 laboratory, while the virus was obtained from ISS (Istituto Superiore della Sanità, Italy). Each viral suspension was prepared and propagated on a large scale in monolayer cell cultures of Vero E6 ATCC CCL-81™ (American Type Culture Collections). Cell cultures were incubated at 37 °C with 5% (v/v) CO<sub>2</sub> in DMEM (Dulbecco's Modified Eagle Medium) added with 10% (v/v) of fetal bovine serum (FBS), 1% (w/v) of penicillin-streptomycin.

Viral titer was calculated using the Spaerman - Karber equation (ID<sub>50</sub> assessment), as follows:

$$-\log_{10}ID_{50} = -(x_0) - \left\{ \left[ \frac{R}{100} \right] - 0.5 \right\} \times -\log_{10} \text{ of the dilution factor} \quad (5)$$

Where  $x_0$  is the 10<sup>th</sup> base logarithm of the lowest dilution with 100% positive reaction and (CPE)  $R$  is the summation (%) of positive cultures.

### *Photo-virucidal test*

The photo-virucidal test was performed at 20° C. A volume of 50 µL of the viral suspension (10<sup>7</sup> PFU/ml) has been inoculated directly on three different samples: a basket ball, a soccer ball and a volley ball. The suspension was allowed to dry and then have been then the sample has been placed inside the irradiation chamber. A 35 mm stainless steel support disc was inoculated with a viral suspension (50 µL) and not irradiated and used as control.

After UVC irradiation (1 min and 2 min), a sterile swab was used to recover the residual virus from sample surface. Thereafter, the swab was inoculated in 1 ml of fresh medium and ten-fold dilutions (from 10<sup>-2</sup> to 10<sup>-9</sup>) were prepared. Each dilution was used to inoculate six wells of 24-well plates containing confluent VERO culture (> 90 %). Six wells of the plate were untreated and considered as controls. Cells were incubated at 37 °C for 1 h, and subsequently the supernatant culture was removed, and cells were washed with PBS and added with fresh medium (500 µl of DMEM supplemented with 2% v/v FBS and 0.75% v/v of carboxymethylcellulose).

After incubation at 37°C for three days, the plaque formation was checked and upon Crystal Violet staining, the infectivity title (ID<sub>50</sub>) was determined with the Spaerman - Kärber equation previously shown (5). A decrease of ≥ 4 log unit of viral titer (pfu/ml) can be considered a virucidal effect.

## Results

### *LED characterization results*

The spectrum of the analyzed LEDs are reported in Figure 2, they have been measured at the nominal current, normalized to the maximum value and plotted in semilog scale. Results indicate that the peak emission wavelength ranges from 275nm for LEDs B1, C1, D1 and 284 nm for LED A2. LED A3 shows an evident higher wavelength emission, thus indicating a possible higher defect density related to Mg acceptors and Nitrogen vacancies [16]. Results of the LED characterized optical power are reported in Figure 3. While LED A2 reports the higher optical power, we focus on the area of around 10 mW to evaluate an LED candidate for the next phase, where B1 and C1 report the higher value for the same current, with a slight advantage for C1.

The results of the electrical characterization are reported in Figure 4, due to their larger chip size, LEDs A2 and A3 show a much lower voltage for the same current. For the other LEDs results are similar up to 100mA, with a  $V_f$  of 5.6V, above this current the higher series resistance of LED C1 has an important effect on voltage drop with respect to D1. Analyzing the efficiency of the LED samples, we detect that the efficiency (Figure 5)

varies between 1 and 3 %. Interestingly LEDs with smaller chip (LED A1) has higher efficiency than bigger LEDs (A2 and A3), the analyzed LEDs have similar efficacy at around 100 mA with values of approx. 1.75 %. All the analyzed LEDs suffer from efficiency droop, but the amount of the droop is strongly dependent on the LED series resistance, for example as seen between B1 and C1. It is also possible to notice that LED B1 has a lower efficiency at lower currents, possibly indicating that a higher defect density increases the non-radiative recombination rate, thus limiting the efficiency at low injection levels [17].

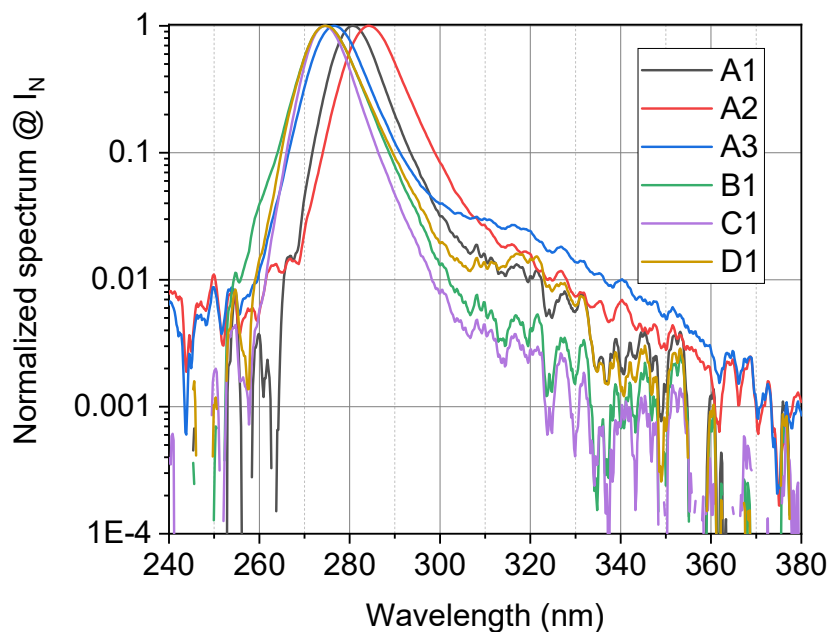


Figure 2: Normalized spectrum of the selected LEDs, semi logarithmic scale, LEDs measured at nominal current, 25°C.

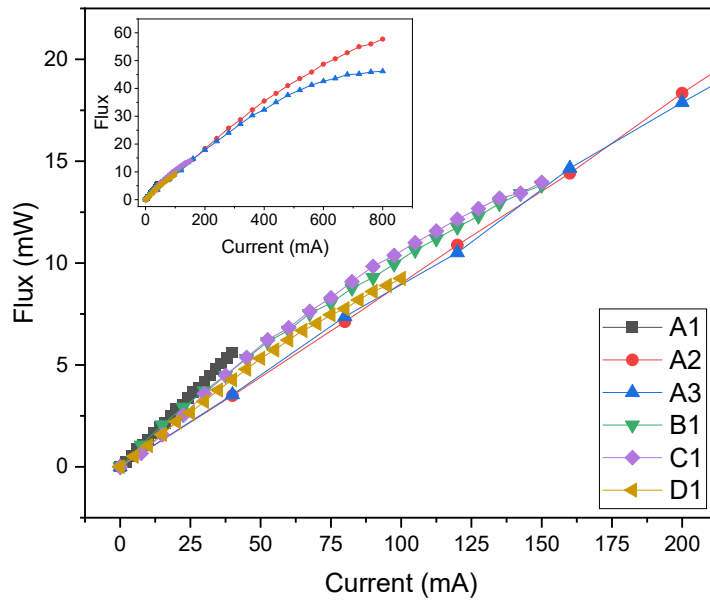


Figure 3: Optical flux as a function of current for the selected LEDs.

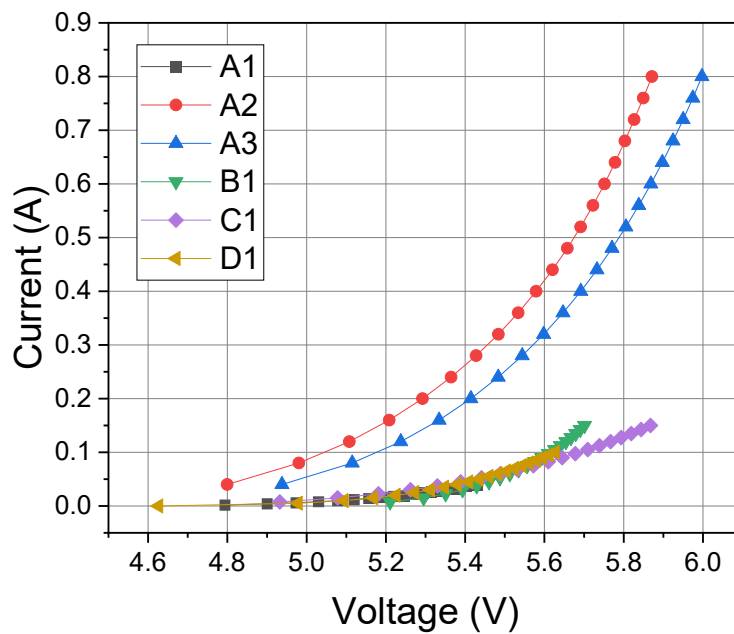


Figure 4: Electrical characteristics of the selected LEDs.

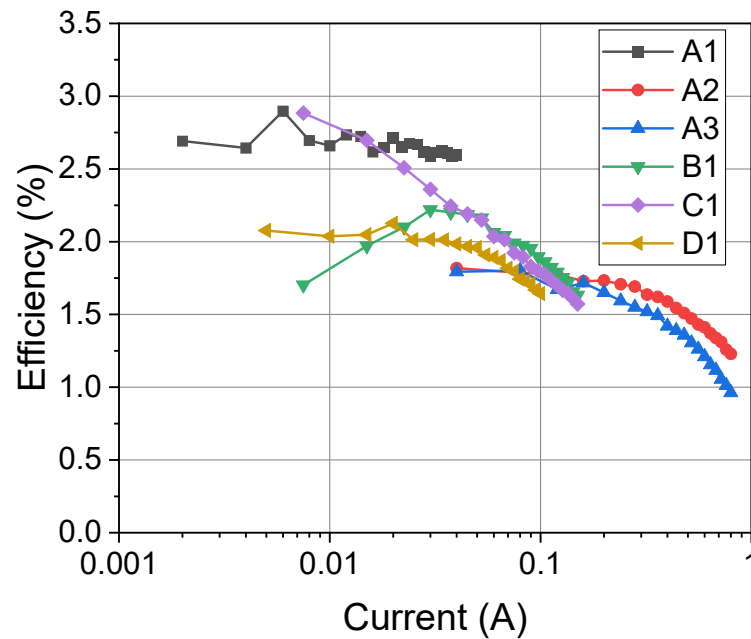


Figure 5: Wall plug efficiency as a function of LED current for the selected samples.

## Design

### LED choice

Based on the previous characterization phase Both LEDs B1 and C1 are good candidates for the design of the system. They have lower emission wavelength, higher OP at around 100 mA with respect to the other candidates. While B1 has higher efficiency and lower voltage, C1 has slightly higher OP. Also due to commercial availability, LED C1 has been chosen for the development of the irradiation system.

### Optical design

The results of the ray tracing simulations are plotted in Figure 6 as the number of LEDs increases, the irradiance becomes more uniform on the target surface. The average irradiance is almost not affected due to the total optical power of the system being fixed at 500 mW in all the simulations. For a quantitative analysis we report in Figure 7 the minimum, average and maximum for the 4 combinations. A massive variation in uniformity is detected between 25 and 50 LEDs, while increasing the number of sources above 50 provide a measurable, but minor improvement.

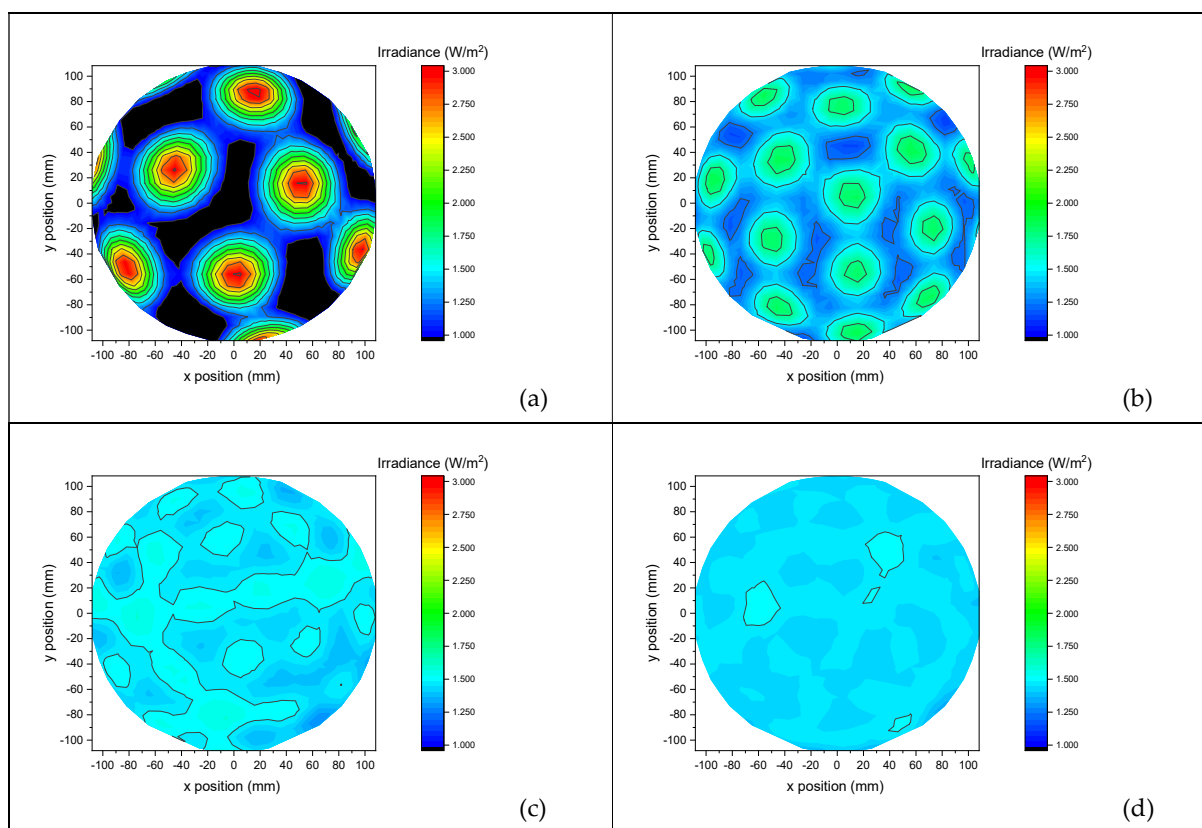


Figure 6: Optical simulation results: irradiance on the surface of the sphere, total optical power is constant at 500 mW, (a) 25 points, (b) 50 points, (c) 75 points, (d) 100 points.

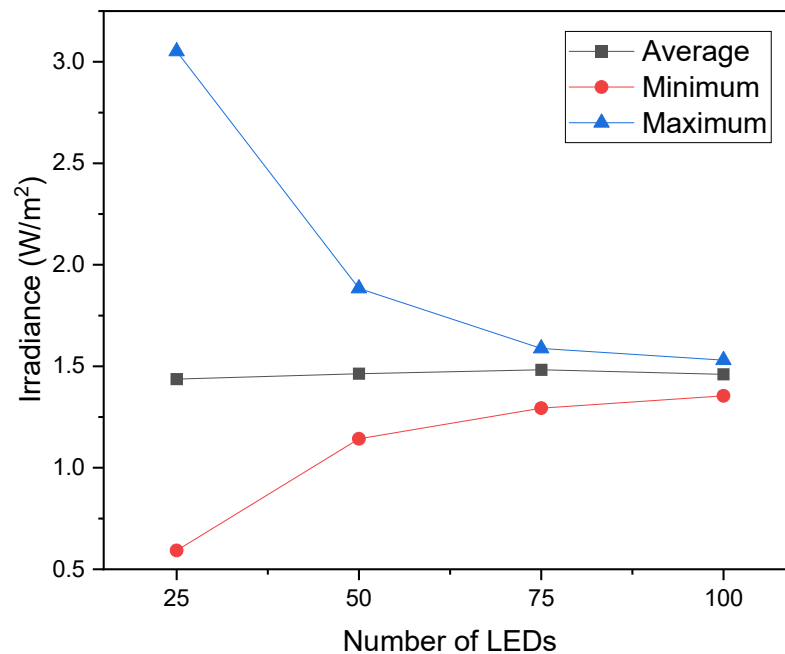


Figure 7: Simulated maximum, minimum and average irradiance as a function of the number of LEDs

#### *Selected optical design*

The design choice has been the use of 56 LEDs, just above the number of 50 as described in the previous section. To allow the subdivision of the sphere in two identical hemispheres with a 330 mm diameter it has been necessary to slightly modify the position of the LEDs, the consequent reduction in the optimized uniformity has been compensated by introduction of 6 more LEDs, bringing the total to 56. The optical power of the single LEDs has been kept at a nominal value of 10 mW, thus allowing a small increase in average irradiance.

For the manufactured prototype it has also been evaluated (Figure 8) the effect of the size of the irradiated sphere, we simulated the irradiance for spheres ranging from 65 mm (the size of a tennis ball) to 250 mm (the size of a basketball) placed at the center of the irradiation chamber. The concentric structure of the system implies that the reduction of the size of the target sphere allows an increase of the average irradiance as well as a reduction of the NU on the surface of the target. The best condition is achieved for a target diameter sphere of 125 mm.

The manufacturing of the prototype has been carried out by means of two-chrome plated identical steel hemispheres. Since a spherical cavity with specular reflectivity would have the effect of guiding the rays which are not incident onto the target surface in a circular loop, a diffused reflectivity has been chosen for the plating process. The effect of diffused reflectivity on the performance of the system has been reported in Figure 9. It can be noticed that as the reflectivity increases the average irradiance increases in a more than linear fashion, the non uniformity of the system therefore reduces. With a chromium reflectivity of approx. 50% in the a non uniformity of 23% is expected at 275 nm.

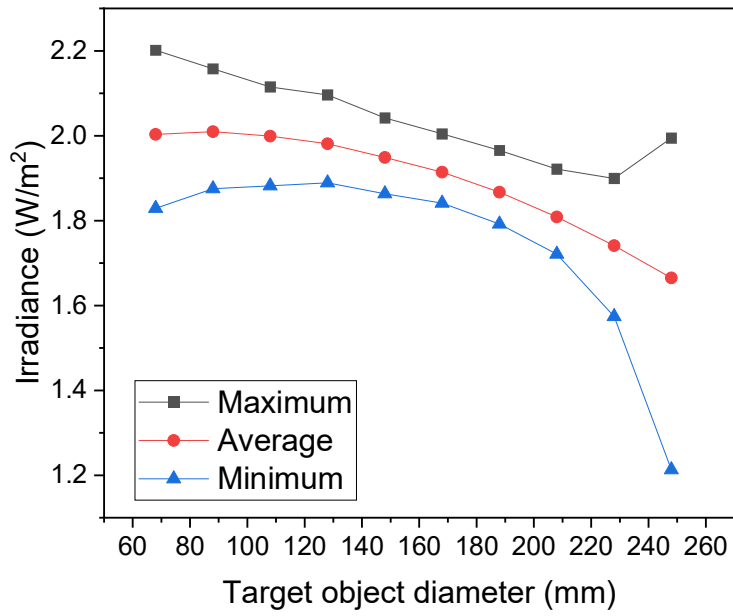


Figure 8: Irradiance as a function of the internal object diameter.

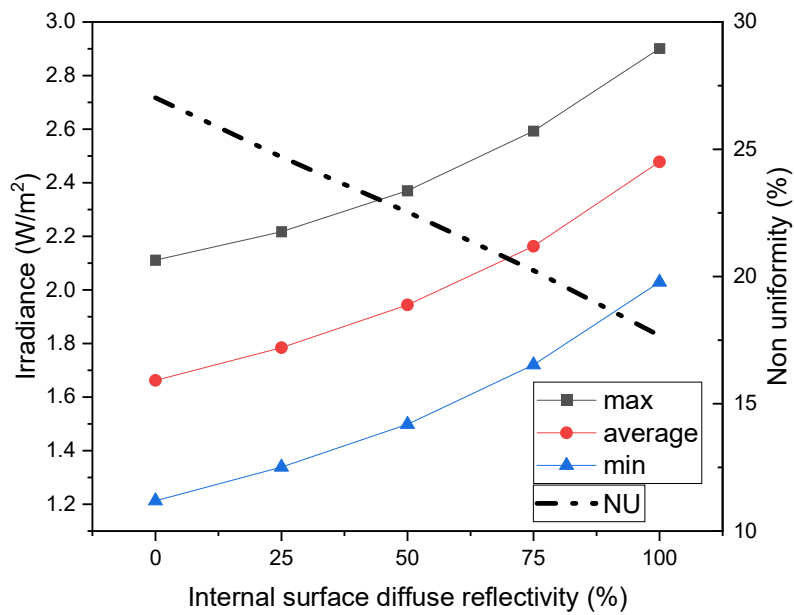


Figure 9: Irradiance and non-uniformity parameter (NU) as a function of internal surface reflectivity

### *Electronic design, safety and robustness*

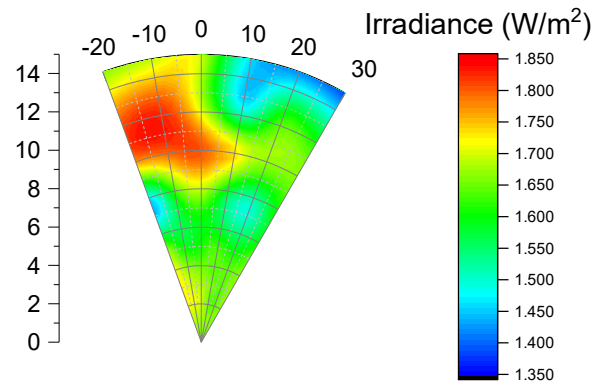
The prototype is driven by standard constant current LED drivers with a high output voltage (up to 200 VDC) allowing the connection of several UVC LEDs in series. The system is regulated and managed by a microcontroller to automate the irradiation process: after the defined irradiation time has elapsed, the LEDs are switched off and the treatment is complete. Since short wavelength light is dangerous both for eyes and skin, when dealing with UVC LEDs maximum care should be taken to avoid accidental human exposure. Both systems are equipped with safety mechanical switches to interrupt the LED circuit and to give feedback to the microcontroller. When the door gets open, the treatment may or may not be completed, the microcontroller resets the timer and when the door is closed it starts over to ensure the designed dose is reached. The system has also been designed to ensure that in case of an LED failure (open circuit or short circuit) the microcontroller detects the voltage variation on the LED chain and reports a failure.

### **Optical characterization results**

The characterization of the prototype reported in Figure 10 has been carried out by a spherical structure with a diameter of 250 mm, the USB4000 spectrometer is encased so that the cosine corrector is tangent to the spherical supporting structure. By rotating the spectrometer support it has been possible to measure the spatial irradiance of a portion of the target surface. Results are presented in Figure 11. The measured minimum irradiance is similar to the simulated value, but since the maximum and average values are slightly lower the NU is down to 13.5% in the sampled area.



Figure 10: Picture of the manufactured prototype with the different tested balls.



Min Irradiance = 1.385 W/m<sup>2</sup>  
 Average Irradiance = 1.64 W/m<sup>2</sup>  
 Max Irradiance = 1.818 W/m<sup>2</sup>

Figure 11: measured uniformity on the surface of a 250 mm sphere wedge.

### Virucidal tests results

The virucidal test results are reported in

Table II, three balls for Soccer, Basketball and Volleyball have been tested. Results indicate that for both 1 and 2 minutes exposure time the percent reduction after test contact time is greater than 99.9%, corresponding to more than log 3 inactivation.

Table II: Results of the SARS-CoV-2 virucidal tests carried out on the surface of different sport balls.

Ball type	Duration of the treatment	Viral titer before treatment*	Viral titer after treatment*	Percent reduction after test contact time
Soccer ball (3 repetitions)	1 min	7.0	0.01	> 99.9 %
	2 min			
basket ball (3 repetitions)	1 min	7.0	0.01	> 99.9 %
	2 min			
Volley ball (3 repetitions)	1 min	7.0	0.01	> 99.9 %
	2 min			

\*Data express the log value of plaque-forming units per milliliter of viral suspension (PFU/ml) at different irradiation times.

### Conclusions

With this work we presented an in dept optical optimization analysis for the design of effective surface treatment systems based on 275nm UVC LEDs, with spherical volume of 18 liters. The light sources are 10mW LEDs emitting at 275nm, which have been selected after an experimental comparison between different manufacturers and solutions. The design target has been the achievement of a minimum level of irradiance, and optimization of the light uniformity: a spherical distribution of 56 LEDs has been chosen, together with a chrome plating treatment of the internal surface of the irradiation chamber.

A prototype of the designed solution has been manufactured, irradiance characterization reported a minimum irradiance of 1.385 W/m<sup>2</sup>.

The antiviral efficacy of the prototype has been demonstrated with respect to Sars-CoV-2 virus by means of specific viral titering before and after the treatment: an

inactivation greater than 99.9% has been detected after 1 minute of exposure. The estimated dose for the treatment, calculated at the minimum irradiance, is 83.1 J/m<sup>2</sup>. The results of this study are of fundamental importance for the design of virus inactivation systems to be used in school and community objects, and can be readily implemented for the realization of UV-C based systems.

## References:

1. Roy, D.; Tripathy, S.; Kar, S.K.; Sharma, N.; Verma, S.K.; Kaushal, V. Study of knowledge, attitude, anxiety & perceived mental healthcare need in Indian population during COVID-19 pandemic. *Asian J. Psychiatr.* **2020**, *51*, 102083, doi:10.1016/j.ajp.2020.102083.
2. Ceylan, R.F.; Ozkan, B.; Mulazimogullari, E. Historical evidence for economic effects of COVID-19. *Eur. J. Heal. Econ.* **2020**, *21*, 817–823, doi:10.1007/s10198-020-01206-8.
3. Stadnytskyi, V.; Bax, C.E.; Bax, A.; Anfinrud, P. The airborne lifetime of small speech droplets and their potential importance in SARS-CoV-2 transmission. *Proc. Natl. Acad. Sci.* **2020**, *117*, 11875–11877, doi:10.1073/pnas.2006874117.
4. Cook, T.M. Personal protective equipment during the coronavirus disease (COVID) 2019 pandemic – a narrative review. *Anaesthesia* **2020**, *75*, 920–927, doi:10.1111/anae.15071.
5. Gondim, J.A.M. Preventing epidemics by wearing masks: An application to COVID-19. *Chaos, Solitons & Fractals* **2021**, *143*, 110599, doi:10.1016/j.chaos.2020.110599.
6. Morten Gram Pedersen, M.M. Data-driven estimation of change points reveals correlation between face mask use and accelerated curtailing of the COVID-19 epidemic in Italy. *COVID-19 SARS-CoV-2 Prepr. from medRxiv bioRxiv* **2020**, doi:https://doi.org/10.1101/2020.06.29.20141523.
7. Fiorillo, L.; Cervino, G.; Matarese, M.; D'amico, C.; Surace, G.; Paduano, V.; Fiorillo, M.T.; Moschella, A.; La Bruna, A.; Romano, G.L.; et al. COVID-19 surface persistence: A recent data summary and its importance for medical and dental settings. *Int. J. Environ. Res. Public Health* **2020**, *17*, doi:10.3390/ijerph17093132.
8. Inagaki, H.; Saito, A.; Sugiyama, H.; Okabayashi, T.; Fujimoto, S. Rapid inactivation of SARS-CoV-2 with deep-UV LED irradiation. *Emerg. Microbes Infect.* **2020**, *9*, 1744–1747, doi:10.1080/22221751.2020.1796529.
9. Asif Khan, M. AlGaIn multiple quantum well based deep UV LEDs and their applications. *Phys. status solidi* **2006**, *203*, 1764–1770, doi:10.1002/pssa.200565427.
10. Shatalov, M.; Jain, R.; Saxena, T.; Dobrinsky, A.; Shur, M. Development of Deep UV LEDs and Current Problems in Material and Device Technology. In: **2017**; pp. 45–83.
11. Trivellin, N.; Monti, D.; De Santi, C.; Buffolo, M.; Meneghesso, G.; Zanoni, E.; Meneghini, M. Current induced degradation study on state of the art DUV LEDs. *Microelectron. Reliab.* **2018**, *88–90*, 868–872, doi:10.1016/j.microrel.2018.07.145.
12. Sárosi, Z.; Knapp, W.; Kunz, A.; Wegener, K. Evaluation of reflectivity of metal parts by a thermo-camera. *InfraMation 2010 Proc.* **2010**, doi:https://doi.org/10.3929/ethz-a-006206911.
13. Semechko, A. Suite of functions to perform uniform sampling of a sphere 2020.
14. Gerchman, Y.; Mamane, H.; Friedman, N.; Mandelboim, M. UV-LED disinfection of Coronavirus: Wavelength effect. *J. Photochem. Photobiol. B Biol.* **2020**, *212*, 112044, doi:10.1016/j.jphotobiol.2020.112044.
15. Hamzavi, I.H.; Lyons, A.B.; Kohli, I.; Narla, S.; Parks-Miller, A.; Gelfand, J.M.; Lim, H.W.; Ozog, D.M. Ultraviolet germicidal irradiation: Possible method for respirator disinfection to facilitate reuse during the COVID-19 pandemic. *J. Am. Acad. Dermatol.* **2020**, *82*, 1511–1512, doi:10.1016/j.jaad.2020.03.085.
16. Trivellin, N.; Monti, D.; Piva, F.; Buffolo, M.; De Santi, C.; Zanoni, E.; Meneghesso, G.; Meneghini, M. Degradation processes of 280 nm high power DUV LEDs: Impact on parasitic luminescence. *Jpn. J. Appl. Phys.* **2019**, *58*, doi:10.7567/1347-4065/ab1393.
17. Kim, M.-H.; Schubert, M.F.; Dai, Q.; Kim, J.K.; Schubert, E.F.; Piprek, J.; Park, Y. Origin of efficiency droop in GaN-based light-emitting diodes. *Appl. Phys. Lett.* **2007**, *91*, 183507, doi:10.1063/1.2800290.